Use of Cold Gas Dynamic Spraying for Repair of Steel Structures

Final Report
April 2021

BRIDGE ENGINEERING CENTER

IOWA STATE UNIVERSITY

Institute for Transportation

About the Bridge Engineering Center

The mission of the Bridge Engineering Center (BEC) is to conduct research on bridge technologies to help bridge designers/owners design, build, and maintain long-lasting bridges.

About the Institute for Transportation

The mission of the Institute for Transportation (InTrans) at Iowa State University is to save lives and improve economic vitality through discovery, research innovation, outreach, and the implementation of bold ideas.

Iowa State University Nondiscrimination Statement

Iowa State University does not discriminate on the basis of race, color, age, ethnicity, religion, national origin, pregnancy, sexual orientation, gender identity, genetic information, sex, marital status, disability, or status as a US veteran. Inquiries regarding nondiscrimination policies may be directed to the Office of Equal Opportunity, 3410 Beardshear Hall, 515 Morrill Road, Ames, Iowa 50011, telephone: 515-294-7612, hotline: 515-294-1222, email: eooffice@iastate.edu.

Disclaimer Notice

The contents of this report reflect the views of the authors, who are responsible for the facts and the accuracy of the information presented herein. The opinions, findings and conclusions expressed in this publication are those of the authors and not necessarily those of the sponsors.

The sponsors assume no liability for the contents or use of the information contained in this document. This report does not constitute a standard, specification, or regulation.

The sponsors do not endorse products or manufacturers. Trademarks or manufacturers' names appear in this report only because they are considered essential to the objective of the document.

Iowa DOT Statements

Federal and state laws prohibit employment and/or public accommodation discrimination on the basis of age, color, creed, disability, gender identity, national origin, pregnancy, race, religion, sex, sexual orientation or veteran's status. If you believe you have been discriminated against, please contact the Iowa Civil Rights Commission at 800-457-4416 or Iowa Department of Transportation's affirmative action officer. If you need accommodations because of a disability to access the Iowa Department of Transportation's services, contact the agency's affirmative action officer at 800-262-0003.

The preparation of this report was financed in part through funds provided by the Iowa Department of Transportation through its "Second Revised Agreement for the Management of Research Conducted by Iowa State University for the Iowa Department of Transportation" and its amendments.

The opinions, findings, and conclusions expressed in this publication are those of the authors and not necessarily those of the Iowa Department of Transportation.

1. Report No.	2. Government Accession No.	3. Recipient's Catalog No.	
IHRB Project TR-758			
4. Title		5. Report Date	
Use of Cold Gas Dynamic Spraying for Repair of Steel Structures		April 2021	
		6. Performing Organization Code	
7. Authors		8. Performing Organization Report No.	
Behrouz Shafei (orcid.org/0000-0001-5677-6324) and Weizhuo Shi (orcid.org/0000-0001-8193-0098)		InTrans Project 18-673	
9. Performing Organization Name and Address		10. Work Unit No. (TRAIS)	
Bridge Engineering Center Iowa State University 2711 South Loop Drive, Suite 4700 Ames, IA 50010-8664			
		11. Contract or Grant No.	
12. Sponsoring Organization Name and Address		13. Type of Report and Period Covered	
Iowa Highway Research Board Iowa Department of Transportation 800 Lincoln Way Ames, IA 50010		Final Report	
		14. Sponsoring Agency Code	
15. Supplementary Notes			
Visit https://bec.iastate.edu for color pdfs of this and other research reports.			

16. Abstract

Several state departments of transportation (DOTs) are facing the daunting task of maintaining an inventory of corroding steel structures. Cold gas dynamic spraying (CS) is an innovative technique that can lead to substantial advances in the repair and retrofit of steel structures subjected to corrosive environments. The CS technique is believed to bring a wide spectrum of benefits, in terms of life-cycle performance and cost, to steel structures currently in service. In addition, the CS technique offers a durable treatment that can be simply applied with a portable device. This significantly expedites the repair process, resulting in minimized road closures and traffic disruptions.

When coated using the CS technique, steel members not only regain their lost structural capacity but also become more resistant to corrosion because the metal coating provides a strong yet passive layer against corrosive environments. This is an important advancement that greatly extends the expected life span of steel structural members without having to repeat maintenance actions every few years.

To achieve the ultimate goal of this exploratory project, a proof-of-concept study was carried out to evaluate the advantages of CS through a set of coupon tests to determine the corrosion resistance of structural steel with and without coating. The outcome not only demonstrates the promise of this emerging technique but can also be used to help tailor the CS process for transportation infrastructure applications for the very first time. This contribution will maximize the impact of this innovative technique, which holds great promise for future use and implementation.

17. Key Words		18. Distribution Statement	
additive manufacturing—cold spray— corrosion test—mechanical properties—structural steel		No restrictions.	
19. Security Classification (of this report)	20. Security Classification (of this page)	21. No. of Pages	22. Price
Unclassified.	Unclassified.	51	NA

USE OF COLD GAS DYNAMIC SPRAYING FOR REPAIR OF STEEL STRUCTURES

Final Report
April 2021

Principal Investigator
Behrouz Shafei, Associate Professor
Bridge Engineering Center, Iowa State University

Co-Principal Investigator
Jonghyun Lee, Assistant Professor
Department of Mechanical Engineering, Iowa State University

Research Assistant
Quin Rogers

Authors
Behrouz Shafei and Weizhuo Shi

A report from
Bridge Engineering Center
Iowa State University
2711 South Loop Drive, Suite 4700
Ames, IA 50010-8664
Phone: 515-294-8103 / Fax: 515-294-0467
https://bec.iastate.edu

TABLE OF CONTENTS

LIST OF FIGURES

LIST OF TABLES

ACKNOWLEDGMENTS

EXECUTIVE SUMMARY

Cold gas dynamic spraying (CS) is a promising additive manufacturing technique in which metallic materials or alloy compounds are deposited onto the surface of a substrate. In CS, an inert gas such as helium or nitrogen is accelerated in a de Laval nozzle through an adiabatic expansion process. CS has mainly been used in the oil and gas industries to apply titanium on metallic substrates. Due to the high price of titanium, one of the aims of the present project was to identify other metallic compounds with the desired corrosion resistance and mechanical performance to be deposited onto corroded steel members using the CS method.

This research project aimed to investigate the feasibility of using the CS method for the repair and retrofit of corroded steel members, especially in bridge structures. This study's outcome is a set of recommendations regarding the use of the cold spray technique in steel structures.

In this study, the experimental program was designed to evaluate the corrosion resistance of cold-sprayed coating on steel coupons. To this end, accelerated corrosion testing was conducted in accordance with ASTM G31 on a variety of metals and alloys, and some were selected for further testing with cold-sprayed coating. Furthermore, the experimental program was designed to investigate the mechanical performance of cold-sprayed steel coupons.

The following key findings resulted from this study:

- From the accelerated corrosion testing, the following conclusions were made:

  1. For the 7-day testing period, the average loss was 4.5% for A36 steel, 5% for A1010 steel, and 10% for aluminum. For the cold-sprayed coupons, the average losses were 4.4% and 1.2% for the coupons coated with Inconel and aluminum, respectively.

  2. For the 14-day testing period, the average loss was 20% for A36 steel, while the average losses were significantly lower for the cold-sprayed coupons coated with Inconel and aluminum, i.e., 4.0% and 3.1%, respectively.

  3. A comparison of the two coating materials investigated revealed that the Inconel-coated bars had higher corrosion rates in both tests and appeared significantly more corroded than the aluminum-coated bars. The aluminum-coated bars had more consistent corrosion, lower corrosion rates, and less severe corrosion, making aluminum the more effective protective coating.

- From the tensile and hardness testing, the following conclusions were made:

  1. It was found that the differences in tensile behavior among the cold-sprayed specimens were not directly related to the coating. This might be because the coated layer was thin for these steel samples.

2. The bonding between the substrate steel and the coating material was found to be in need of attention after the steel began to yield.

3. From the hardness testing, the cold-sprayed steel coupon coated with Inconel had a Rockwell A hardness value of 77.5. However, the Rockwell A hardness value of the cold-sprayed steel coupon coated with aluminum was found to be 11.2 because the aluminum coating significantly softened the material.

INTRODUCTION

Background

A growing investment is made every year in the repair and replacement of deteriorating structures. For steel structures in particular, corrosion is the main cause of deterioration and adversely affects the long-term integrity and performance of this category of structures, in addition to the consequences of extreme loading events (Arabi et al. 2018, 2019; Arabi and Shafei 2019; Shurbert-Hetzel et al. 2021, Shi et al. 2021).

Cold gas dynamic spraying (CS) is a promising additive manufacturing technique in which metallic materials or alloy compounds are deposited onto the surface of a substrate. In CS, an inert gas such as helium or nitrogen is accelerated in a de Laval nozzle through an adiabatic expansion process (Koivuluoto and Vuoristo 2014). Depending on the initial temperature, pressure, and type of the gas, the gas's velocity can reach up to two or three times the speed of sound (i.e., 1,000–1,200 m/s) (Assadi et al. 2016). When micron-sized particles (10–70 µm in diameter) are introduced either upstream or downstream of the nozzle, they are entrained by the high-speed gas of reduced temperature.

Since the powder feedstock remains well below its melting temperature, CS is categorized as a solid-state deposition method. Consequently, CS can minimize or eliminate the deleterious effects inherent in conventional thermal spraying (TS) methods, including thermally induced residual stresses, melting, oxidation, phase transformation, decomposition, and grain growth (Raoelison et al. 2017). Motivated by the development of nonmelting deposition techniques, experimental and analytical studies have been performed to provide an in-depth understanding of the bonding mechanism(s) in CS. It has been revealed that adhesion can be fully achieved when the powder particles exceed the so-called critical impact velocity during the CS process (Grujicic et al. 2003, Schmidt et al. 2009a, Bae et al. 2009, Moridi et al. 2013). The critical impact velocity is substantially dependent on the particle and substrate material properties (Stoltenhoff et al. 2002, Li et al. 2013), as well as environmental conditions such as temperature and pressure (Li et al. 2007, Yin et al. 2012). Such information has been documented in the literature for various materials and environments, which has helped users of this technology customize the spraying parameters and optimize manufacturing costs.

A schematic of the CS system that was used in the present project is shown in Figure 1.
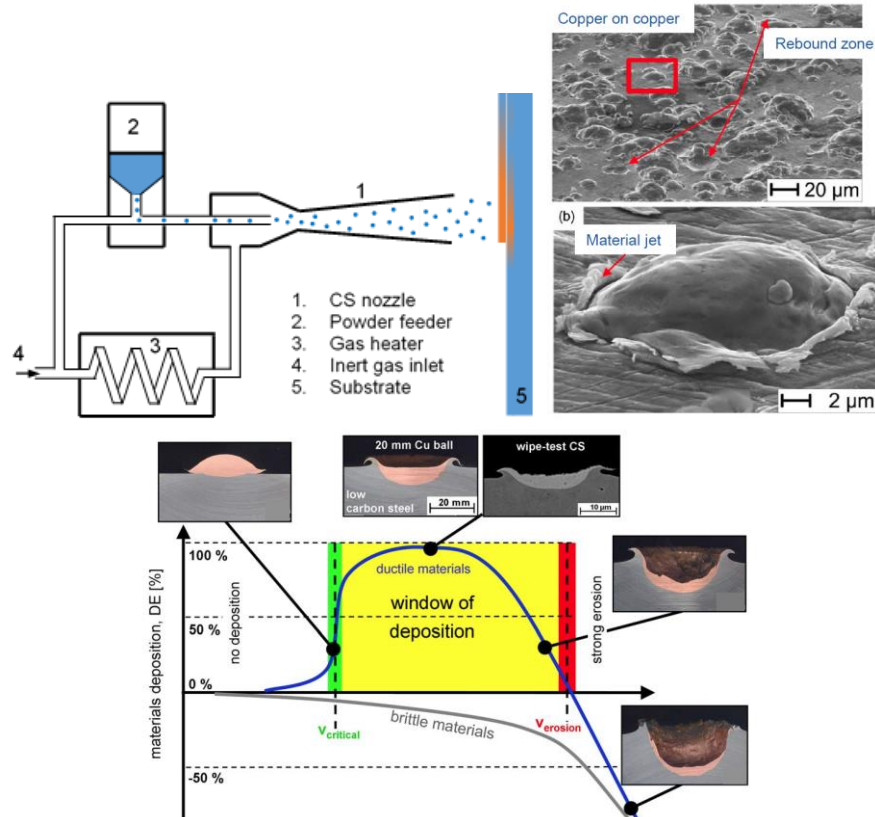
Schmidt 2009, Open Access provided by the Springer Nature SharedIt content-sharing initiative

Figure 1. Schematic presentation of cold spray setup (top left), microscopic view of the material jet resulting from cold spraying (top right), and window of deposition for ensuring ductile performance (bottom)

CS has mainly been used in the oil and gas industries to apply titanium on metallic substrates (Wang et al. 2007, Sun et al. 2008, Binder et al. 2010, Wong et al. 2011, Prisco et al. 2018). Due to the high price of titanium, one of the aims of the present project was to identify other metallic compounds with the desired corrosion resistance and mechanical performance to be deposited onto corroded steel members using the CS method.

In a few recent research studies, the CS technique has been used successfully to apply copper and stainless steel coating to the outer surface of a steel canister for a nuclear fuel repository (Coddet et al. 2015, Fernandez et al. 2016). The layer deposited on the steel using the CS technique exhibited superior mechanical and chemical properties, comparable to those of wrought copper and bulk stainless steel. This demonstrated the effectiveness of cold-sprayed copper and stainless steel coatings in structural applications. Since both copper and stainless steel are considered noble metallic materials with a reactivity to oxygen significantly lower than that of steel, it is believed that they can be promising choices for further consideration.

2

Research Objective and Scope

The primary goal of the work presented in this report was to investigate the feasibility of using the CS method for the repair and retrofit of corroded steel members, especially in bridge structures. To this end, a holistic experimental program was established that included accelerated corrosion tests, hardness tests, and mechanical tests. First, the optimal cold spray parameters (e.g., gas pressure, gas temperature, particle temperature, and substrate temperature) were determined and documented. Next, the corrosion resistance of CS coating on steel coupons was evaluated for various exposure times. The mass loss values of the corrosion specimens provided essential information on the serviceable lifetime of cold-sprayed steel coupons. Finally, tensile tests were performed to study the restoration of the structural capacity of corroded steel coupons after CS coating.

It is anticipated that the outcome of this project will build on the capacities developed to date in the rapidly growing domains of additive manufacturing and robotic construction. This contribution will maximize the impact of this innovative method, which holds great promise for future use and implementation.

Report Organization

This final report consists of six additional chapters, along with a References section:

- **Literature Review (Chapter 2)**. This chapter presents a literature review whose goal was to determine the optimal cold spray parameters (e.g., gas pressure, gas temperature, particle temperature, and substrate temperature).
- **Cold Spray Manufacturing Process (Chapter 3)**. This chapter documents the manufacturing process used to apply cold spray coatings to substrate materials.
- **Accelerated Corrosion Testing (Chapter 4)**. This chapter presents an evaluation of the corrosion resistance of CS coating on steel coupons using accelerated corrosion tests with various exposure times.
- **Experimental Testing (Chapter 5)**. This chapter presents a study on the restoration of the structural capacity of corroded steel coupons after CS coating. This was examined through tensile tests.
- **Summary and Conclusions (Chapter 6)**. This chapter summarizes the content of the report and provides conclusions and recommendations.

LITERATURE REVIEW

Introduction

This review of the cold spray method is divided into three sections. The first section reviews the coating formation mechanism, including the cold spray manufacturing system, the required temperature and pressure, the coating materials, and the deposition process. The second section reviews the benefits and performance of cold spray coatings that provide corrosion protection. The third section reviews studies on the mechanical properties of both the deposited material and the combined coating and substrate system.

Coating Formation Mechanism

Cold spraying is a type of additive manufacturing, meaning that a part gets built up from a substrate rather than trimmed down from a larger component. Some other types of additive manufacturing are flame spraying, high-velocity oxygen fuel (HVOF) spraying, high-pressure gas spraying, plasma spraying, laser spraying, and detonation spraying. HVOF and plasma spraying are commonly used. Typically, various types of thermal spraying melt powders down during the spraying process. This causes high residual stresses from rapid cooling and commonly causes oxide coatings to form. Cold spraying occurs at temperatures considerably lower than the melting temperature of the powder, meaning that the powder stays in its solid state throughout the deposition process, which avoids the negative aspects of other deposition processes (Borchers et al. 2008, Raoelison et al. 2017). The goal of cold spraying is to produce a dense and nonporous coating.

The cold spray system is made up of many components: a high-pressure gas supply, a gas control system, a gas heater, powder feedstock with a powder feed gas system, and a spraying chamber/workstation that includes a nozzle and substrate with an appropriate motion system (Bala et al. 2014, Raoelison et al. 2017). The substrate is typically a solid metal, but other materials such as ceramics and glass are occasionally used. Nitrogen gas is used most often, followed by helium, which has high operational costs. Free air is sometimes used, but it contains oxygen, increasing the likelihood that oxides will form (Bray et al. 2009, Assadi et al. 2016, Oyinbo and Jen 2019). These gases are heated to temperatures up to 1,000°C and pressurized to 25 to 40 bars (Raoelison et al. 2017). This means that the gas and powder combination leave the nozzle at a speed between 600 and 1,200 m/s (Bray et al. 2009, Kim et al. 2009, Hassani-Gangaraj et al. 2015, Assadi et al. 2016, Oyinbo and Jen 2019).

The temperature and pressure that the gas is heated to has a large impact on the coating quality. Villa et al. (2013) completed a study where they deposited 316L stainless steel (SS) powder onto an aluminum alloy substrate at a variety of temperatures and pressures to determine which conditions were most effective for creating a dense and nonporous coating. Test results showed that temperature had the largest impact on coating quality. Low temperatures (600°C) created coatings with low cohesion that were also porous. High temperatures (800°C) allowed for dense coatings to be made, and the quality and deposition efficiency of the coating increased with

pressure. The highest quality coating was created at the highest temperature and pressure, 800°C and 40 bars.

The coating material particles used in cold spraying can range in size from less than 1 to 50 μm, and the low temperatures allow for temperature-sensitive materials to be used (Kim et al. 2009). Metals, metal alloys, and metal matrix composites are the most commonly used materials. Metal matrix composites are a mix of metals and nonmetals such as ceramics, polymers, and nanostructures (Silva et al. 2016). The size of the particles is an important factor to consider. Spencer and Zhang (2011) completed an experimental study to determine how the porosity of the coating would be affected by the particle sizes used. They theorized that a range of particle sizes would result in the densest coatings. They deposited 316L austenitic SS powder onto a magnesium substrate with helium gas heated to 320°C and a gas exit speed of 1,245 m/s. The test results showed that powders with particles of a single small size (<20 μm) resulted in the fewest pores but introduced some operational problems. Mixed sizes of particles resulted in low porosity with little to no operational problems.

Laser-assisted cold spraying (LACS) is essentially the same as cold spraying except the gases are heated to lower temperatures and the particles are primarily heated through a strong laser focused at the deposition area on the substrate. This allows for lower operational costs and higher safety due to considerably decreased temperatures (as low as 450°C). The pressures used in LACS are comparable to those used in cold spraying, on average 10 to 30 bars (Bray et al. 2009).

To complete the cold spraying, a pre-heated gas is channeled through the nozzle. For most systems, the powder is mixed with pre-heated gas in a mixing chamber before meeting the higher speed gas in the nozzle, and the mixture is then sprayed 5 to 25 mm to be deposited onto the substrate (Oyinbo and Jen 2019, Bala et al. 2014). The nozzle is a converging-diverging de Laval nozzle, which normally has an exit area of 10 to 15 mm^2.

The deposition process is quite complex and is not entirely understood. The simplified mechanism that is often used to describe how coatings are formed is that high velocities and temperatures lead to the plastic deformation of particles, creating a bond between the spray and the substrate (Villa et al. 2013). This is not incorrect, just very simplified. The collision between the particles and the substrate is comparable to the behavior of particles in explosive powder compaction, where shock waves are used to combine powder into a dense solid by undergoing plastic deformation (Borchers et al. 2008, Assadi et al. 2016). The particles undergo strain rates of about 107 to 109 s^{-1} (Spencer and Zhang 2011, Kim et al. 2009). For particles to be deposited, they need to reach their critical velocity. This velocity is impacted by many factors, some of which include particle size, hardness, temperature, and pressure. If the velocity is lower than this, the particles tend to bounce off and erode the substrate, and if it is higher the particles can melt onto the substrate, which is undesirable (Kim et al. 2009). Deposition efficiency can be used to indicate the number of particles that have an impact velocity higher than their critical velocity and can be calculated with the following equation:

$$DE = \frac{\Delta S_w}{\sum P_w} \qquad (1)$$

where DE is deposition efficiency, ΔS_w is the weight change of the sample, and P_w is the theoretical deposited mass with 100% deposition efficiency (Villa et al. 2013).

Spencer et al. (2012) completed an experimental study where they researched the effect of Al_2O_3 in SS powder as a cold spray coating. The hypothesis was that having harder and softer materials in the coating would allow for higher deposition efficiency. The authors proposed a deposition mechanism where the nondeformable particles (Al_2O_3) would create higher localized strain in the deformable particles (SS) and the Al_2O_3 particles would take up space on the surface, causing fewer oxides to form, all of which would result in higher metallic bonding. Tests were completed with different Al_2O_3 concentrations in SS powder. The test results showed an increase in deposition efficiency with the inclusion of Al_2O_3, suggesting that the authors' proposed mechanism was correct.

Bonding between particles occurs when the surfaces of those particles touch. Metal particles tend to have oxide coatings, so for bonding to occur these coatings must be removed or broken. Solid-state bonding, which occurs in cold spraying, shows four common characteristics: bonding occurs above the critical velocity, bonding depends on the particle impact angle, bonding results from adiabatic shear instabilities (ASI), and bonding is associated with extremely high plastic strains, which are shown by dynamic recrystallization. Particles tend to bond better when the impact angle is close to perpendicular, and the chance of bonding decreases as the angle moves away from 90° (Assadi et al. 2016).

Adiabatic shear instability is found at the particle/substrate interface and is a result of strain hardening due to the particles' impact and thermal softening due to plastic work on the particles. As the particle material moves laterally, shear stresses are generated and stay in the particles. This manifests as jets that form at the interface, shown in Figure 2.
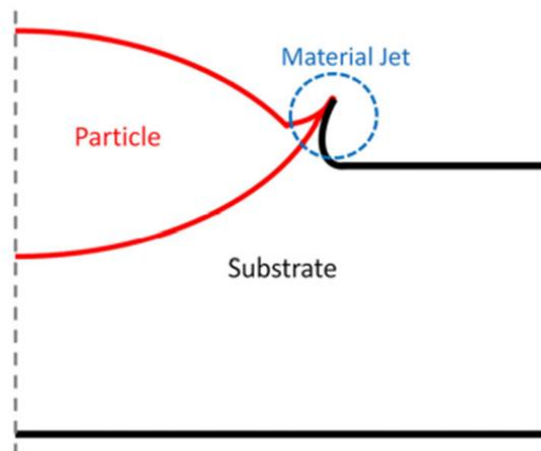
Schematic deformation of particle and substrate in cold spray deposition
Hassani-Gangaraj et al. 2015, rights managed by Taylor & Francis

Figure 2. Material jet formation

These jets form at the edges of the particles and include both particle and substrate materials. The ASI is impacted by many parameters, including the density, strength, melting temperature, and specific heat of the materials. It is also more prominent in larger particles. The ASI zone starts from the outside of the particles and works inward, seldom reaching the centers of the particles. The ASI zone is essential to bonding, and the larger the area, the stronger the bond (Hassani-Gangaraj et al. 2015, Assadi et al. 2016).

Bonding in cold spraying can be divided into two parts: adhesion with the substrate material and build-up of the coating. Adhesion is determined by metallurgical bonding. Metallurgical bonding occurs during particle impact when structural changes or transformations are made to the particle, bonding the particle to the substrate material (Raoelison et al. 2017, Oyinbo and Jen 2019). Dynamic recrystallization occurs alongside the ASI zone as a partner to metallurgical bonding. Dynamic recrystallization occurs when part of the particle is dominated by a change in temperature rather than external stresses. As particles heat up due to collision, metal particles re-align, which is visible as grain refinement near the particle/substrate interface. The mechanism for dynamic recrystallization is not entirely known and is often not included in cold spraying models due to its complex nature (Raoelison et al. 2017). Three specific bonding mechanisms have been identified in adhesion: interfacial mixing, embedment in the substrate, and anchoring of particles. Interfacial mixing is the most complex; it consists of complex deformation resulting in swirling zones at the particle/substrate interface. It is not considered a primary mechanism in cold spraying (Raoelison et al. 2017). Embedment in the substrate occurs when the spray particles have a higher hardness than the substrate and individual spray particles adhere to the substrate via embedment. Anchoring of particles is like embedment, but it occurs when the substrate is not ductile. In this case, deposited particles tend to sit on top of the substrate with weak bonds (Raoelison et al. 2017).

The build-up of the coating consists of ductile or nonductile deposition. Ductile deposition occurs in most cold spraying scenarios where metals are used. After the adhesive first layer is formed, three stages of ductile deposition follow (Raoelison et al. 2017, Oyinbo and Jen 2019). First, the impacting particles meet with the base layer, rotating and deforming the base layer and improving the bond to the substrate. As more particle layers are formed, plastic deformation occurs in the lower layers, decreasing the porosity of the system and creating bonds between particles. This continues until the coating is complete, the final stage being densification and further hardening.

Nonductile deposition occurs when particles break during collision, causing highly angular fractured pieces to bond with the substrate and with each other. The high angularity creates strong cohesion. Nonductile deposition tends to occur with ceramics (Raoelison et al. 2017, Oyinbo and Jen 2019).

Silva et al. (2016) conducted research on the effectiveness of Al_2O_3 and Al coatings on carbon steel in improving corrosion and wear resistance. Al_2O_3 was deposited on top of a thin Al layer on the substrate surface to achieve a better bond. Scanning electron microscope (SEM) and optical microscope (OM) analyses of these coatings showed plastic deformation of individual particles, leading to strong bonds and very low porosity (<0.8%). The coating was found to have

denser core layers, with more porosity occurring toward the edges of the coating. This is consistent with the current understanding of cold spray coating formation described above. Tests also confirmed that no changes in chemical composition took place after deposition. Adhesion to the substrate and the density of the coatings improved with an increase in temperature and pressure.

These different types of deposition can be seen in the microstructures of cold spray coatings. The three primary microstructural features found in cold spray coatings are severe plastic deformation, signified by dislocations and other defects; grain refinement due to dynamic recrystallization, shown near the particle/substrate interface; and nonbounded interfaces, generally at the center of impact zones (Assadi et al. 2016).

Borchers and Partners (2008) compared the microstructure of cold spray powders and coatings to that resulting from explosive powder compaction. In both cold spray and explosive powder compaction, the microstructure changed from body-centered cubic (bcc) to face-centered cubic (fcc). The microstructures for 316L SS coatings were quite uniform, in contrast to copper coatings, which showed nonuniform microstructures. Adiabatic shear instabilities and jet formations were found as proof of bonding. Interparticle welding was found throughout the coating as well. Some older sources identify flash welding from impact as the source of particle bonding (Bray et al. 2009).

Corrosion Protection

One of the biggest problems in achieving long-life concrete and steel structures is steel corrosion. Steel corrosion occurs in many forms, including uniform, pitting, crevice, and galvanic corrosion (Koivuluoto and Vuoristo 2014). Corrosion of a steel member means a reduction of its cross-sectional area, which reduces its tensile strength. For this reason, it is desirable to reduce corrosion. Cold spraying a corrosion-resistant material onto a steel substrate has shown success in preventing this problem.

Many substances are used to create cold spray coatings. Bala et al. (2014) provides an extensive table that compiles data from many studies and gives a thorough description of coatings (metals, alloys, etc.) and their best uses. The most common substances used are zinc, aluminum, glassy coatings, and titanium. Zinc creates a protective layer by having a negative corrosion potential, meaning the zinc will corrode before the steel substrate. Aluminum creates an oxide layer, preventing the substrate material from corroding through inhibited kinetics (Koivuluoto and Vuoristo 2014). Glassy coatings are amorphous and have strong chemical homogeneity. This prevents corrosion by not allowing the formation of galvanic cells, which are the cause of pitting corrosion. Cold-sprayed titanium is more effective at preventing corrosion than carbon steel and adds many mechanical benefits to the steel. Common substrates that are used in cold spray coatings to provide corrosion protection are steel, aluminum, and magnesium alloys (Hassani-Gangaraj et al. 2015).

Applying corrosion protection coatings through cold spraying has some drawbacks. Porosity is one of the biggest factors that affects corrosion resistance, regardless of coating material. The

more porous the coating, the deeper water and chlorides can reach into the coating, making it less effective at preventing corrosion. It is therefore very important to reduce the porosity of cold spray coatings. A common way to do this is to heat treat the cold-sprayed item, which can reduce pores and surface oxides and reduce the corrosion current factor by 7 to 10. The particle size used can affect the porosity and thus the corrosion resistance. Larger particles tend to leave more pores, whereas finer particles can compact more with fewer pores, leading to higher corrosion resistance (Hassani-Gangaraj et al. 2015).

Sundararajan et al. (2008) conducted a study in which 316L stainless steel particles were cold sprayed on a carbon steel substrate and the effects of heat treatment on the corrosion resistance of the coated samples were tested. The stainless steel particles used in the cold spray were up to 15 μm in size and were sprayed using compressed air at a temperature of 475°C and a pressure of 2.0 MPa. Three heat treatments were tested, one at 400°C, one at 800°C, and one at 1,100°C, and the specimens were allowed to cool in the air after being held at their respective temperature for 1 hour. The specimens were then submerged in a 0.1 N HNO_3 solution for 1 or 24 hours, and the polarization resistance and corrosion potential were measured. The test results showed that increasing the heat treatment temperature decreased the corrosion rate to the point where the 1,100°C samples had corrosion rates very close to that of bulk 316L stainless teel. Without heat treatment, the coating was still effective at decreasing corrosion in the substrate material.

Laser treatments are also used on occasion, replacing or supplementing heat treatment. Laser treatments have been shown to improve bond quality and reduce interparticle boundaries. These boundaries are preferential corrosion sites (Hassani-Gangaraj et al. 2015). One study looked at the effectiveness of laser treatment on titanium cold spray coatings. The study found that the nontreated coating did not provide much corrosion protection, but the laser-treated specimens had corrosion rates comparable to that of bulk titanium (Olakanmi and Doyoyo 2014).

Another way to control the porosity of the coating is to alter the deposition temperature and pressure. Across all coating materials, the general trend is that increasing deposition temperature improves corrosion resistance to a certain point. The initial temperature increase leads to an increase in cohesive strength and decreased porosity, improving corrosion resistance. After a certain point, however, the corrosion resistance begins decreasing, which can be attributed to a higher degree of plastic deformation of the coating particles and a change in the chemical potential of the metal atoms. Hassani-Gangaraj et al. (2015) found that increasing the deposition temperature of stainless steel from 450°C to 500°C changed the corrosion rate from 0.47 to 0.02 mm/year. Increasing the deposition temperature of titanium from 600°C to 800°C decreased the porosity to almost half and increased the corrosion resistance by an order of magnitude.

The gases used also have some impact on corrosion resistance. Helium gas can produce more corrosion-resistant coatings than nitrogen gas (Hassani-Gangaraj et al. 2015). The ability to control oxygen content in the coating through the gas (air, helium, nitrogen) can also increase corrosion resistance (Villa et al. 2013).

Using more than one substance (co-depositing metals, alloys, and/or ceramics) in a coating has shown conflicting effects on corrosion resistance. It appears that using hard particles to tamp

metallic particles can decrease porosity, increasing corrosion resistance, but the interface between the hard and metallic particles is subject to local corrosion (Hassani-Gangaraj et al. 2015). Some studies have shown that adding Al_2O_3 to Al cold spray on a magnesium alloy substrate showed no improvement in corrosion resistance (Bala et al. 2014).

Spencer et al. (2012) conducted an experiment testing the effectiveness of adding Al_2O_3 to 316L stainless steel powder to be cold sprayed onto a magnesium alloy substrate. Powders were mixed at 25%, 50%, and 75% Al_2O_3 by volume, with the other percentage containing stainless steel powder. The Al_2O_3 powder particles had an average size of 20 μm, and the stainless steel powder particles had an average size of 7 μm. Helium gas was used at a pressure and temperature of 620 kPa and 320°C, respectively. Corrosion resistance was tested using a neutral salt spray test and electrochemically using potentiodynamic anodic polarization in a neutral 5% NaCl solution. The salt spray tests were completed following ASTM B117 for 168 hours. The test results showed that the Al_2O_3 created a sufficient bond with the substrate, and no corrosion on the substrate was seen. Increasing the Al_2O_3 content reduced the change in noble potential between the coating and the substrate, meaning an increased corrosion resistance.

Silva et al. (2016) conducted a similar study, focusing on the effectiveness of adding Al_2O_3 to an aluminum coating on a low-carbon steel alloy to protect against corrosion and improve wear resistance. In this study, the Al_2O_3 was added as a layer on top of a base Al layer rather than spraying the two together as a mixture. The Al powder particles were round with an average particle size of 28 μm, and the Al_2O_3 particles were angular in shape with an average particle size of 63 μm. The powders were deposited via nitrogen gas at a pressure of 25 bars and a temperature of 350°C. Both powders were sprayed simultaneously from separate powder feeds, allowing the Al powder to be deposited onto the substrate and the Al_2O_3 powder to be deposited onto the Al layer. The feed ratio of Al to Al_2O_3 was 3:1. The coating was found to be effective at protecting the substrate from corrosion in all 3,000-hour salt fog tests. The coating showed higher corrosion resistance than a pure Al coating when immersed in NaCl solution. The results showed that the Al_2O_3 coating was more effective than an Al coating at resisting corrosion.

Mechanical Performance

The cold spraying process has a large impact on the mechanical properties of both the deposited material and the combined coating and substrate system. Some of these mechanical properties are hardness, tensile strength, fatigue strength, wear resistance, and shear strength. The values of many of these properties change in the sprayed material due to the extreme plastic deformation the particles undergo. The values of some properties decrease due to the deformation, such as ductility (Assadi et al. 2016). The values of others increase, such as elastic modulus (Olakanmi and Doyoyo 2014). The interfaces between particles and between the particles and the substrate are the main sources of failure, and the mechanical properties are strongly influence by these interfaces (Assadi et al. 2016). One way to attain more desirable mechanical properties is to decrease the mean particle size of the powder used, increasing the particles' deposition velocity and creating stronger bonds within the coating (Coddet et al. 2015).

Tensile strength is very important in most metal applications, and a cold spray coating can have an impact on this. Coddet et al. (2015) studied the effect of different deposition pressures on the mechanical properties of 304L stainless steel cold spray coatings. The coatings were deposited onto AISI 4130 steel cylinders, which had been grit-blasted before coating. The cold spray consisted of stainless steel particles with an average diameter of 30 μm and was applied using helium gas at 550°C. The two tested pressures were 23.1 and 27.9 bars. Some samples were heat treated in air for 4 hours at temperatures ranging from 200°C to 1,050°C before quenching in water. In the high-pressure samples with no heat treatment, the ultimate tensile strength was high (629 to 525 MPa), but samples failed brittlely. The low-pressure samples had ultimate tensile strengths around 228 MPa. This difference is due to the stronger interparticle bonds created at higher pressures, and both samples had tensile strengths lower than bulk 304L stainless steel. Figure 3 shows the effects of heat treatment on the samples cold-sprayed at 28 bars. The figure shows how heat treatment increased the maximum strain significantly but decreased the maximum tensile stress.
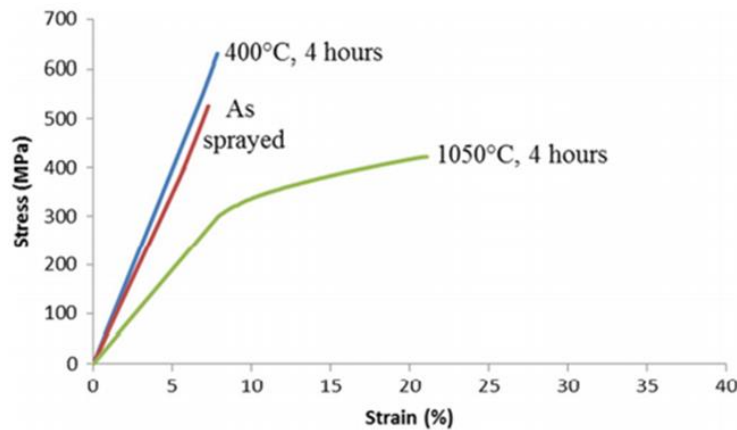
Figure 3. Typical stress-strain curves of deposits sprayed at a nozzle pressure of about 28 bars (CS28) in as-sprayed and annealed conditions

Al-Mangour et al. (2013) completed a study on the effects of different cold spray parameters on the mechanical performance of the coating. These parameters included gas type, temperature, and heat treatment. 316L stainless steel powder was deposited onto a mild carbon steel substrate. Nitrogen gas was used at 700°C and helium gas was used at 350°C, both at a pressure of 4 MPa. The heat treatments consisted of specimens being heated to a temperature ranging from 400°C to 1,100°C for 1 hour, then air cooled. Microhardness tests were completed using a Vickers microhardness apparatus with a load of 0.98 N, with at least 10 measurements taken per sample. Tensile tests were completed on an MTS 810 Materials Testing System with a strain rate of 10^{-3} s^{-1}. The microhardness test results showed that the helium-sprayed samples, including the as-sprayed samples, had higher microhardness values for nearly all temperatures, as shown in Figure 4.
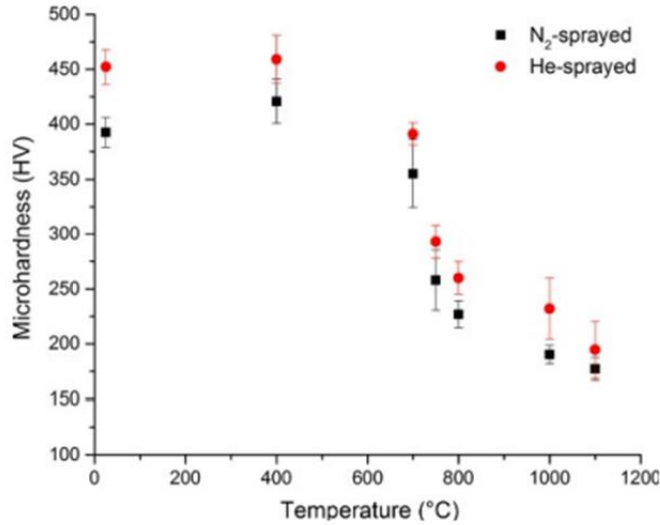
Figure 4. Variation in microhardness as a function of heat treatment temperature

The microhardness profile of both the helium- and nitrogen-sprayed samples had four stages: (1) no change up to 400°C, (2) a gradual decrease from 400°C to 700°C because of the beginning of recrystallization, (3) a sharp decrease from 700°C to 800°C because of recrystallization, and (4) a considerably slowed rate of decrease in hardness above 800°C due to the completion of recrystallization. The nitrogen-sprayed samples had low tensile strength and ductility in the as-sprayed state and when heat treated to 400°C. Strength and ductility increased at both 800°C and 1,000°C but decreased at 1,100°C due to grain coarsening. The helium-sprayed sample in the as-sprayed state had a tensile strength about double that of the nitrogen sample, but due to experimental errors only one specimen was tested. The samples at 1,000°C and 1,100°C had lower tensile strength and ductility values. The tensile strengths in all scenarios were lower than that of bulk 316L stainless steel. Figure 5 shows the tensile strengths of each heat treatment temperature in comparison to bulk 316L stainless steel, as well as a comparison of the ultimate tensile strength and elongation at failure for coatings sprayed with nitrogen or helium and heat treated at different temperatures.
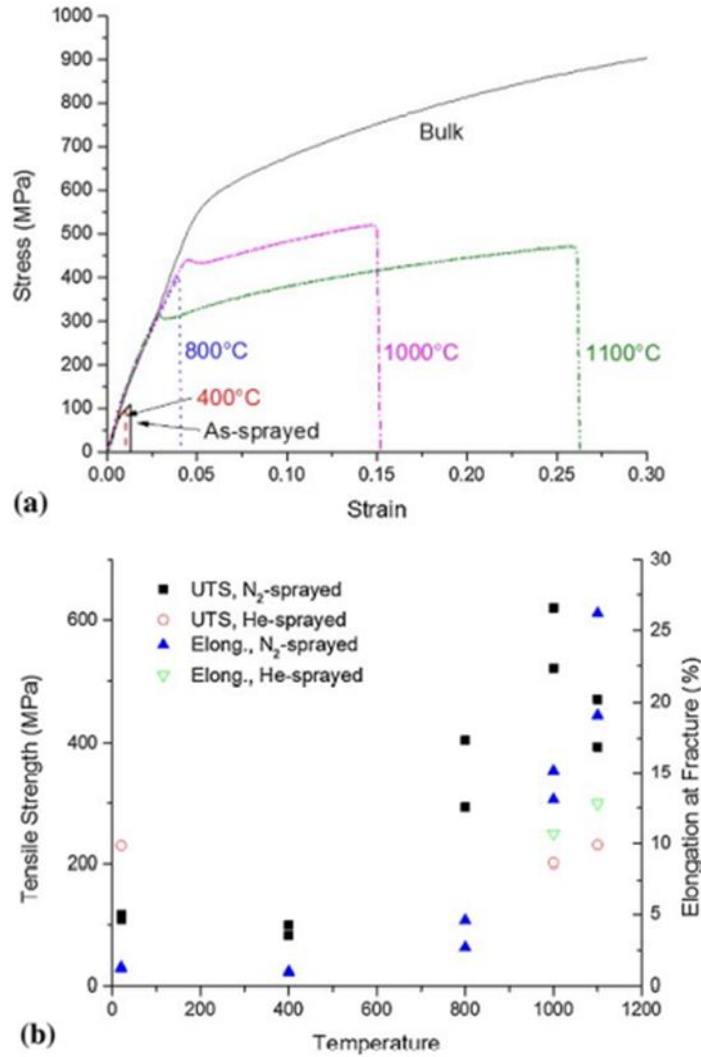
Figure 5. (a) Stress-strain curves for N₂-sprayed coatings and (b) tensile strength and elongation at fracture data for N₂- and He-sprayed coatings with heat treatment

The figure shows higher ultimate tensile strength and elongation at failure for nitrogen-sprayed samples compared to helium-sprayed samples at the same treatment temperature.

The shear strength of coatings is another crucial factor. Some metals, such as titanium, have shown a significant increase in shear strength when applied in a cold-sprayed coating (Hassani-Gangaraj et al. 2015). Spencer et al. (2012) conducted an experimental study focused on the corrosion behavior of stainless steel and Al_2O_3 coatings and tested the shear strength, wear resistance, and hardness of the cold-sprayed coating. (The coating application is described in the Corrosion Protection section above.) The microhardness testing was done using a 200 g load, with indent diagonals between 25 and 30 μm. The tests were repeated using a Vickers hardness tester with a 5 kg load. Wear testing was completed by polishing samples and then using a grinder with a load of 3 N and a linear speed of 20 cm/s. Last, shear bond strength tests were completed on 10×10×40 mm strips with a 1 mm cold spray coating. The strips were forced

13

through a die with a 10×10 mm opening using a tensile testing machine until the coating was removed. The test results showed that the Vickers hardness of the coating increased with increasing Al_2O_3 content, as shown in Figure 6.

Figure 6. Vickers hardness of stainless steel cold spray coatings as a function of Al_2O_3 content

The wear rate decreased with increasing Al_2O_3 content. The Al_2O_3 content had no clear effect on the shear strength of the coatings.
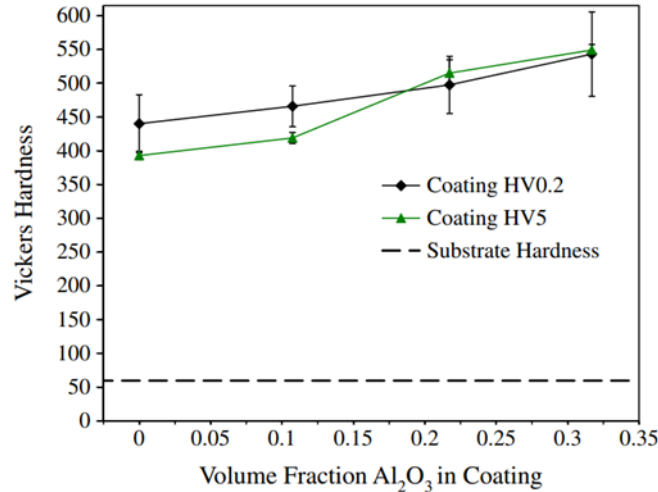
Villa et al. (2013) investigated the efficiency of different cold spray parameters on the wear resistance of the cold spray coating. 316L stainless steel powder with an average particle size of 31.5 μm was deposited onto 7075-T6 aluminum alloy at different temperatures and pressures using nitrogen gas. A rubber wheel test following ASTM G65-04 was completed to measure wear reisistance, and microhardness and nanohardness were measured following ASTM E384-11e1. The test results showed the best wear resistance for the sample with the highest temperature and pressure (800°C and 40 bars), and this wear resistance was about 300% higher than that of the substrate. The coating had a hardness almost double the hardness of the initial powder under optimal deposition conditions.

Silva et al. (2016) studied the effects of adding Al_2O_3 to Al powder that was cold sprayed onto a carbon steel substrate with the goal of improving mechanical performance and corrosion resistance. The Al_2O_3 powder was deposited on top of an Al layer that had been sprayed on the substrate using nitrogen gas at 350°C and 25 bars. Microhardness was tested with a Vickers apparatus following ASTM E384-99. Two wear tests were completed: ball-on-disk following ASTM G99-04 and rubber wheel following ASTM G65-00. The test results showed that adding Al_2O_3 increased the sliding wear resistance. The rubber wheel test showed similar wear rates between the Al and Al/Al_2O_3 coatings. The coating with Al_2O_3 had a 22% higher microhardness, but this could have been due to more optimized spraying conditions.

Adding a cold-sprayed coating to a substrate can improve the fatigue strength of the specimen. Some composites, such as nanostructured powders and metal matrix composites, can increase the fatigue strength of the system (Raoelison et al. 2017). Ziemian et al. (2014) tested the effect of shot peening and glass bead grit blasting on the mechanical properties of Al-2024-T351 aluminum alloy substrate with an aluminum cold spray coating. The cold spray powder had a mean particle size of 20 to 35 μm and was deposited using nitrogen gas at 230°C and 3.45 MPa. Fatigue testing was completed in accordance with ISO 1143. Grit-blasted specimens with cold spray coating had the best fatigue performance at stress levels of 210 and 180 MPa, as shown in Figure 7.
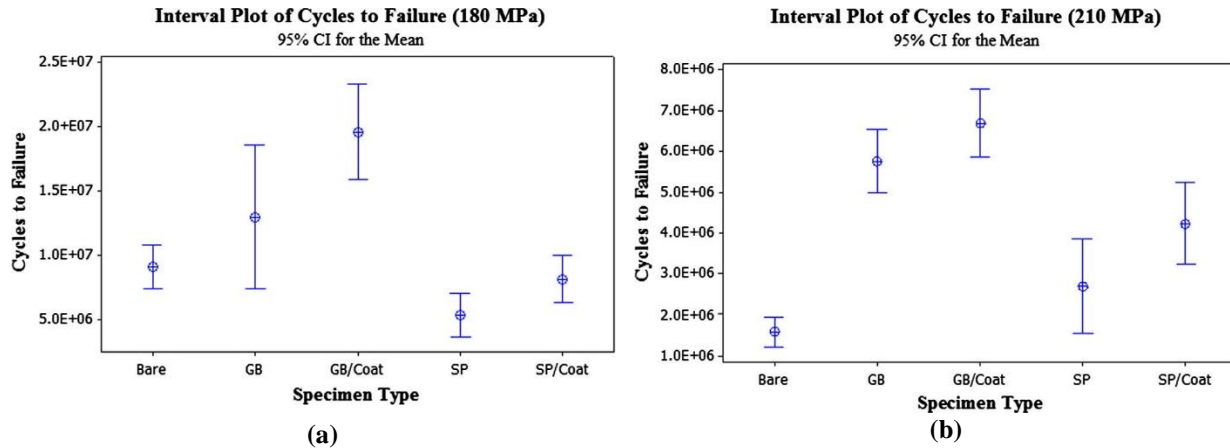
Figure 7. Fatigue life results at different stress levels: (a) 180 MPa and (b) 220 MPa

As the figure shows, the uncoated, untreated specimens had the lowest number of cycles to failure. The grit-blasted, coated samples had a fatigue life over 800% longer than the lowest fatigue life. At 180 MPa, the uncoated, shot-peened specimens had the lowest number of cycles to failure. Coated specimens that had been surface prepared lasted 40% to 50% longer than uncoated specimens, depending on the applied stresses.

COLD SPRAY MANUFACTURING PROCESS

CS is a method of particle deposition achieved through the high-velocity impinging of micron-sized solid particles on a substrate. Bonding between the substrate and coating materials is due to a combination of metallurgical bonding and mechanical interlocking. CS is considered a thermal spray method but is performed at temperatures well below the melting points of the substrate and coating materials so that both the powder and the substrate remain in a solid state. The efficacy of CS is highly dependent on multiple parameters, as documented in Table 1.

Table 1. List of CS parameters

Item	Parameter
Powder/substrate material	Consider ductility and hardness
Powder diameter	5–50 µm (15–45 µm typ.)
Gas	Nitrogen, Helium
Gas pressure	1,000–1,200 psi (1200 psi preferred)
Temperature	300°C–750°C
Particle velocity	Up to 1,200 m/s
Angle of application	Perpendicular for best results
Substrate surface condition	Varies

Effect of Materials on Adhesion

Ductile materials are preferred for CS. Brittle materials alone are unlikely to adhere on impact. However, composite powders containing a sufficient percentage of a ductile material can allow the use of brittle substances, such as ceramics, for coating. The hardness of the substrate and coating materials affects the result as well. For CS applications involving similar materials for both the coating and substrate, the hardness typically only affects the critical velocity (i.e., the velocity required for adhesion). When dissimilar materials are used, the impacting particles must be harder than the substrate material for the proper formation of a CS coating.

Powder Processing

The coating powders are processed and stored in an inert gas (typically argon) to prevent oxidation. It is important to note that any oxidation that occurs on the particles due to exposure during the CS process is eliminated through their impact with the substrate.

Substrate Preparation

Flat and nearly flat surfaces result in the greatest deposition efficiency and the lowest porosity coatings. The best CS results occur with abrasive surface preparation. This treatment provides an interface with no oxide layer and only pure metal. Sharp contrasts in the surface will likely produce poor results.

Cold Spray Systems

Both permanent and mobile CS systems are available. Most systems are contained in booths to isolating the surrounding area from the sound and dust generated by the CS process. Heavy-duty air filtration is used for these facilities.

ACCELERATED CORROSION TESTING

Accelerated corrosion testing was conducted in accordance with ASTM G31 on a variety of metals and alloys, and some were selected for further testing with cold-sprayed coating. This chapter summarizes the procedure used to evaluate the electrochemical corrosion of immersed steel specimens, including specimen preparation, the testing apparatus used, the testing conditions, and the methods used to clean the specimens, and provides an evaluation of the results.

Accelerated Corrosion Testing Setup

The experiment described in this chapter sought to replicate one of two types of corrosion commonly found in structural steel: pitting corrosion. Pitting corrosion is caused by chloride ion attack, which usually results from de-icing salts or marine spray either seeping into the concrete to reach the rebar or in some way being present on the surface of the structural steel. In contrast, uniform corrosion in steel is caused by carbon dioxide breaking down the thin iron oxide layer that otherwise prevents corrosion. In pitting corrosion, chloride ions create small areas of anodes and cathodes on the surface of the steel, causing parts of the steel to be eaten away (Imperatore et al. 2017).

The initial chemical reactions that take place during corrosion are as follows:

$$Fe \rightarrow Fe^{2+} + 2e^- \tag{2}$$

$$4e^- + 2H_2O + O_2 \rightarrow 4OH^- \tag{3}$$

Equation 2 shows how iron is removed from the metal as it dissolves into the electrolytic solution. Equation 2 shows the anodic reaction, and Equation 3 shows the cathodic reaction. The reactions above show how imposing an electrical current, i.e., increasing the concentration of electrons, can force corrosion to occur faster following Le Chatelier's principle. This is the process used in the experiment described below.

Additional chemical reactions take place to create reaction products:

$$Fe^{2+} + 2OH^- \rightarrow Fe(OH)_2 \tag{4}$$

$$4Fe(OH)_2 + O_2 + 2H_2O \rightarrow 4Fe(OH)_3 \tag{5}$$

$$2Fe(OH)_3 \rightarrow Fe_2O_3 \cdot H_2O + 2H_2O \tag{6}$$

Equation 4 shows an intermediary corrosion product that goes on to react with oxygen and water to form ferric hydroxide in Equation 5. Dehydrated ferric oxide, which is the product of Equation 6, is commonly known as rust and forms when water is removed from the corrosion products. In

accelerated corrosion testing, rust does not form because the metal samples stay covered by water during the entire corrosion process.

Specimen preparation and cleaning roughly followed ASTM G31 but did not include chemical cleaning. The corrosion specimens were prepared as coupons with two thicker ends and a thinner center portion with a hole drilled close to one end. All samples were dimensioned in accordance with ASTM E8 standard. The mass of each sample was collected, and each specimen was labeled by stamping it with a number. A copper wire was stripped and connected to each sample through the hole. Teflon tape was attached around the ends, followed by tar tape and electrical tape to seal the electrical connection.

The types of metal selected for laboratory testing included aluminum, ASTM A1010 corrosion-resistant steel, and ASTM A36 steel. The dimensions of the coupons are shown in Figure 8, Figure 9, and Figure 10.
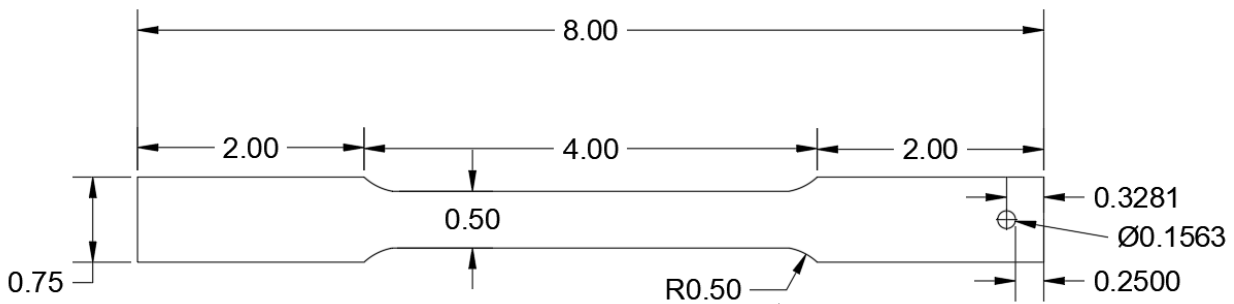

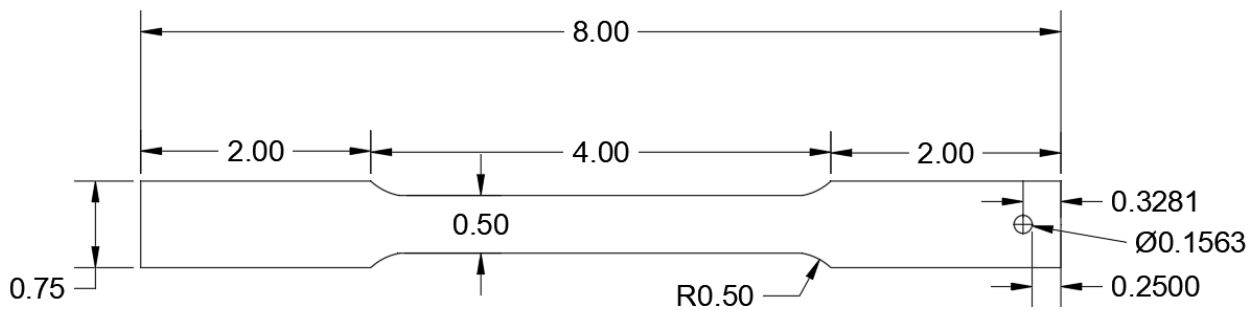**Figure 8. Steel coupon dimensions for aluminum sample (inches)**

Figure 9. Steel coupon dimensions for ASTM A1010 sample (inches)
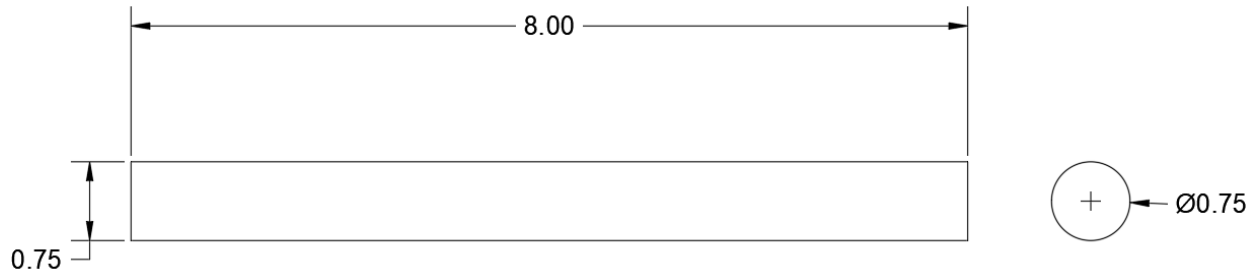
Figure 10. Steel coupon dimensions for ASTM A36 sample (inches)

The specimens were corroded in 34-quart clear plastic tubs filled with 3.5% saltwater by mass. The metal pieces were placed on plastic blocks to allow water to reach the entirety of the sample. The corrosion of the specimens was accelerated by impressing an anodic current of 0.07 A. This was done through an integrated system that incorporated a DC rectifier with a built-in ammeter to monitor the current. In corrosion testing, the amperage used determines the rate of corrosion; higher amperage means more mass loss.

In each plastic tub, the specimen served as the anode and a piece of steel rebar placed alongside the specimen served as the cathode. This arrangement was enforced by the direction of the current. In the first tub, the rebar was connected to the positive output of the power supply and the sample was connected to the rebar of the next container. A schematic representation of the accelerated corrosion test setup is shown in Figure 11, and images of the test in progress are shown in Figure 12.
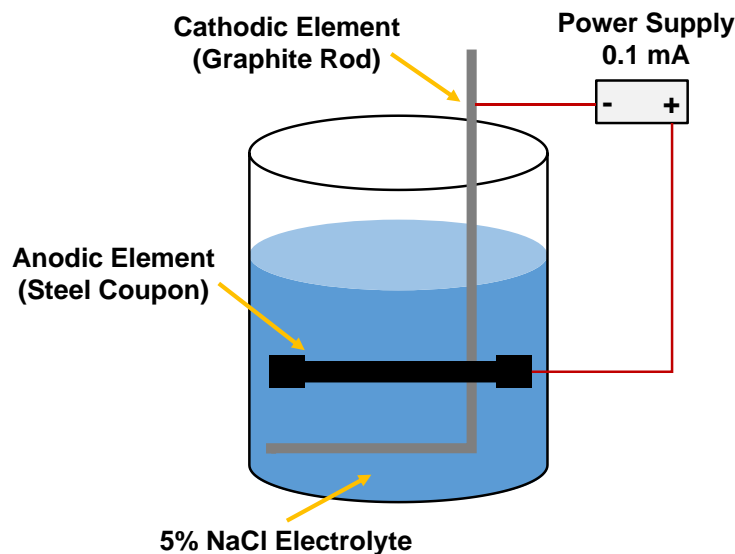
Figure 11. Schematics of the circuit used in the accelerated corrosion test

(a)
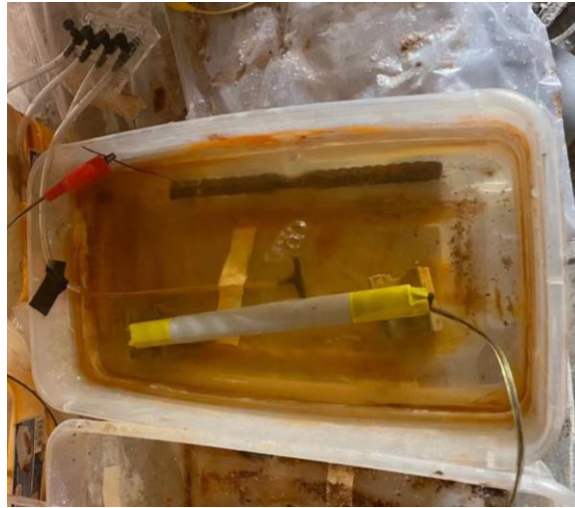
(b)

Figure 12. Accelerated corrosion test setup: (a) A36 steel specimens and (b) cold spray specimens

In order to maintain a consistent current throughout the tubs, the amper value supplied to each batch of testing was checked on a regular basis, and any drift was corrected. This pattern was continued until the last container, where the specimen was connected to the negative output of the power supply.

Compressed air was used along with plastic tubing and aerators to ensure sufficient oxygen in the water of each tub. All corrosion occurred at an ambient air temperature (around 70°F). Samples were checked regularly to ensure the setup was functioning properly. The corroded ASTM A36 samples, A1010 samples, and aluminum samples are shown in Figure 13, Figure 14, and Figure 15.

(a)

(b)

Figure 13. Corroded ASTM A36 specimens: (a) average 20% mass loss and (b) average 5% mass loss

Figure 14. ASTM A1010 corrosion samples

Figure 15. Aluminum samples

Accelerated Corrosion Results

After the specified amount of time for corrosion, generally 7 or 14 days, the power supply was shut off, and the samples were removed from the saltwater solution. All of the tape was removed, and the samples were cleaned in water with a metal bristle brush to gently remove any corrosion products and then dried. After drying, the samples were weighed, and the mass loss was calculated as a percentage using Equation 7.

$$\frac{Initial\ mass - Final\ mass}{Initial\ mass} \times 100\% \tag{7}$$

The corroded samples for A36 steel (4.5% and 20% mass loss), A1010 steel, and aluminum were analyzed, and the results are documented in Table 2, Table 3, Table 4, and Table 5.

Table 2. Corrosion degrees of the artificially corroded A36 steel samples (5% mass loss)

Specimen ID	Weight measurement		Mass loss (%)
	Initial (g)	Day 7 (g)	
1	457	436.1	4.6
2	456.8	437.2	4.3
3	456.3	436.8	4.3
4	456.5	436.9	4.3
5	456.9	436.4	4.5
6	456.7	437.1	4.3
Average	456.7	436.8	4.4

Table 3. Corrosion degrees of the artificially corroded A36 steel samples (20% mass loss)

Specimen ID	Weight measurement		Mass loss (%)
	Initial (g)	Day 12 (g)	
1	454.1	367.0	19.2
2	452.5	362.8	19.8
3	451.9	368.5	18.5
4	453.9	368.3	18.9
5	456.4	366.6	19.7
6	454.2	357.4	21.3
7	453.9	355.9	21.6
8	453.7	353.6	22.1
9	456.3	360.4	21.0
10	454.4	357.4	21.4
11	454.6	350.6	22.9
12	453.8	357.2	21.3
13	453.8	355.2	21.7
14	453.8	357.3	21.3
15	454.2	356.2	21.6
16	455.8	355.2	22.1
17	453.6	350.3	22.8
18	452.5	358.8	20.7
Average	454.1	358.8	21.0

Table 4. Corrosion degrees of the artificially corroded A1010 steel samples (5% mass loss)

| Specimen ID | Weight measurement | | Mass loss (%) |
	Initial (g)	Day 7 (g)	
1	331.3	312.7	5.6
2	326.9	308.1	5.8
3	330.5	314.1	5.0
4	329	311.0	5.5
5	328.1	308.8	5.9
6	328.9	311.3	5.4
Average	329.1	311.0	5.5

Table 5. Corrosion degrees of the artificially corroded aluminum samples (10% mass loss)

| Specimen ID | Weight measurement | | Mass loss (%) |
	Initial (g)	Day 7 (g)	
1	54	48.9	9.4
2	54	49.1	9.1
3	54.1	48.9	9.6
4	54	49.1	9.1
5	53.9	49.5	8.2
6	54.1	48.6	10.2
Average	54.0	49.0	9.3

After the initial corrosion process, the corroded samples were repaired using cold spray coatings (i.e., aluminum and Inconel), as shown in Figure 16.

Figure 16. Corroded samples with the mass lost due to corrosion repaired using cold spray coating

As the figure shows, the mass loss due to corrosion could be completely replaced with the coating. Tensile tests were conducted to investigate the mechanical properties of the samples with and without corrosion and cold spray coating. The process and results for the accelerated corrosion testing conducted on samples with cold spray coating are discussed in the following section, and the tensile testing process and results are discussed in the next chapter.

Accelerated Corrosion Results for Cold-Sprayed Steel Coupons

Corrosion tests were performed on the steel bars with Inconel or aluminum cold spray coatings by submerging the bars in saltwater and running a 0.07A current through the system for a set period. The mass loss for each specimen, representing the amount of corrosion occurring on the metal bar, was calculated. The results are shown in Table 6 and Table 7.

Table 6. Seven-day test results for steel coupons with cold spray coating

	Inconel	Aluminum
Initial mass	486.21 g	462.59 g
Final mass	464.60 g	456.93 g
Mass loss (%)	4.4%	1.2%
Mass loss per day	3.09 g/day	0.81 g/day

Table 7. Fourteen-day test results for steel coupons with cold spray coating

	Inconel	Aluminum
Initial mass	474.75 g	466.08 g
Final mass	455.81 g	451.67 g
Mass loss (%)	4.0%	3.1%
Mass loss per day	1.35 g/day	1.03 g/day

Before and after photos of the metal bars subjected to 7-day corrosion testing are shown in Figure 17 for the coupons coated with Inconel and Figure 18 for the coupons coated with aluminum.

Figure 17. Seven-day before and after photos, Inconel

Figure 18. Seven-day before and after photos, aluminum

Similarly, before and after photos of the metal bars subjected to 14-day corrosion testing are shown in Figure 19 for the coupons coated with Inconel and Figure 22 for the coupons coated with aluminum.
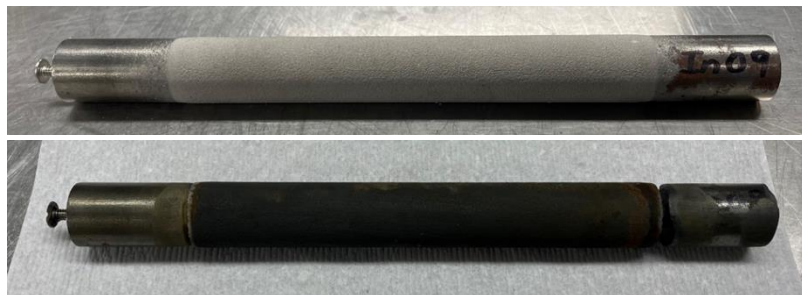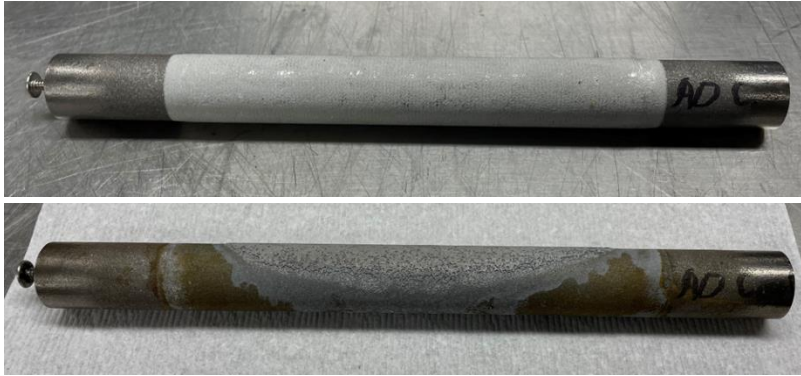

Figure 19. Fourteen-day before and after photos, Inconel

Figure 20. Fourteen-day before and after photos, aluminum

The Inconel-coated bars had higher corrosion rates in both tests and appeared significantly more corroded than the aluminum-coated bars. The coating remained, but the base steel was eaten away, leaving the cold spray coating ineffective, as shown in Figure 21.
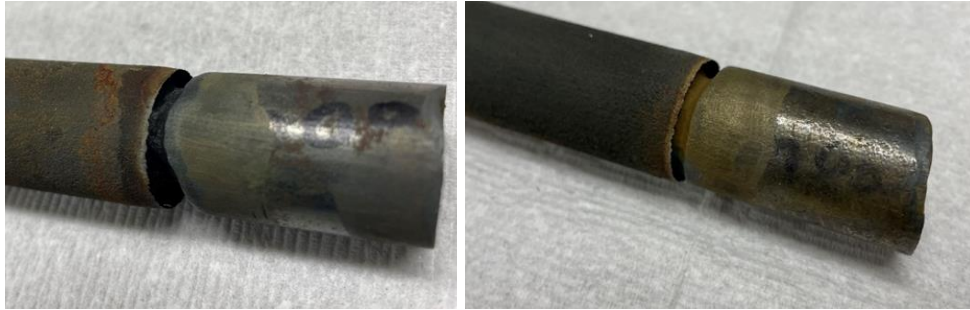

Figure 21. Closeup of corrosion on Inconel bars after 7-days (left) and 14-days (right)

In comparison, the aluminum-coated bars had more consistent corrosion, lower corrosion rates, and less severe corrosion, making aluminum the more effective protective coating.

Accelerated Corrosion Test Summary and Conclusions

The experimental program described in this chapter was designed to evaluate the corrosion resistance of cold-sprayed coating on steel coupons. To this end, accelerated corrosion testing was conducted in accordance with ASTM G 31 on a variety of metals and alloys, and some were selected for further testing with cold-sprayed coating.

From the accelerated corrosion testing, the following conclusions were made:

- For the 7-day testing period, the average loss was 4.5% for A36 steel, 5% for A1010 steel, and 10% for aluminum. For the cold-sprayed coupons, the average losses were 4.4% and 1.2% for the coupons coated with Inconel and aluminum, respectively.

- For the 14-day testing period, the average loss was 20% for A36 steel, while the average losses were significantly lower for the cold-sprayed coupons coated with Inconel and aluminum, 4.0% and 3.1%, respectively.

- It was also found that the Inconel-coated bars had higher corrosion rates in both tests and appeared significantly more corroded than the aluminum-coated bars. The aluminum-coated bars had more consistent corrosion, lower corrosion rates, and less severe corrosion, making aluminum the more effective protective coating.

EXPERIMENTAL TESTING OF MATERIAL AND MECHANICAL PROPERTIES

The experimental techniques performed to investigate the material and mechanical properties of the steel coupons coated with cold-sprayed aluminum and Inconel are described in this chapter. The testing program included hardness measurement and tensile tests.

Tensile Tests

To determine tensile strength properties, such as yield strength, ultimate tensile strength, and elongation at fracture, the tests were conducted under a monotonic loading scenario. The geometry of coupon samples was designed following the standard test method according to ASTM E8 (2018), which was the same as that used for the corroded samples. The test set up is shown in the MTS loading machine, and its associated system was used for tensile testing, as shown in Figure 22. For each specimen, an extensometer (clipped on the sample) was used to determine the strain rate during the testing.
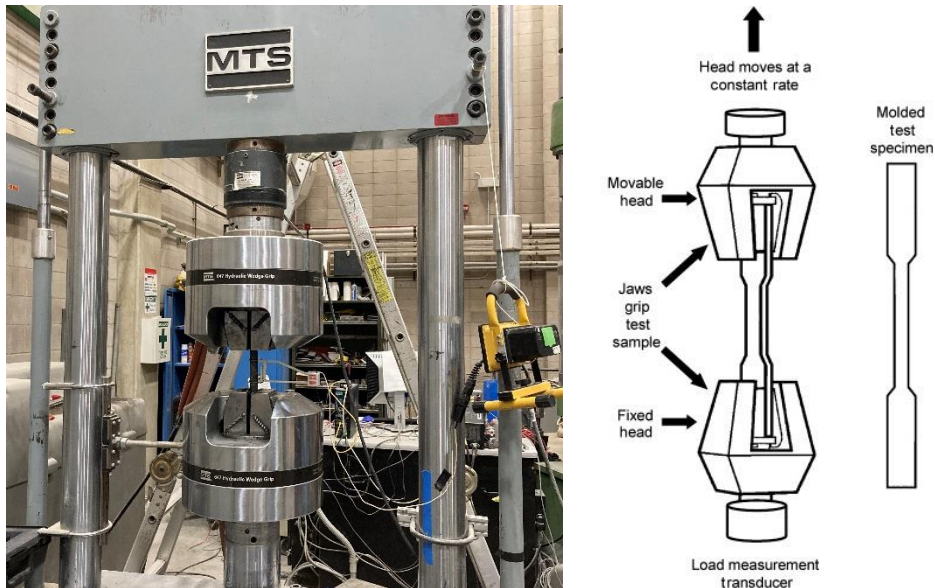

Figure 22. Tensile testing setup

Table 8 documents the average yield strength, elongation, and modulus of elasticity for each specimen.

Table 8. Tensile testing results

Coupon ID	Yield strength (ksi)	Tensile strength (ksi)	Modulus of elasticity (ksi)	Elongation (%)	Note
A36	54	77	29,748	32.0%	-
A36-C (5)	50	72	25,061	24.8%	Corroded (5% loss)
A36-C (20)	30	46	15,000	21.3	Corroded (20% loss)
CSAl	55	78	27,500	33%	Coating with Al on uncorroded A36 steel
CSIn	57	74	28,500	34%	Coating with In on uncorroded A36 steel
CSAl-C	38	44	18,706	10.1%	Coating with Al on corroded A36 steel
CSIn-C	23	27	17,078	5.3%	Coating with In on corroded A36 steel

The load-displacement behavior is presented in Figure 23, Figure 24, and Figure 25.
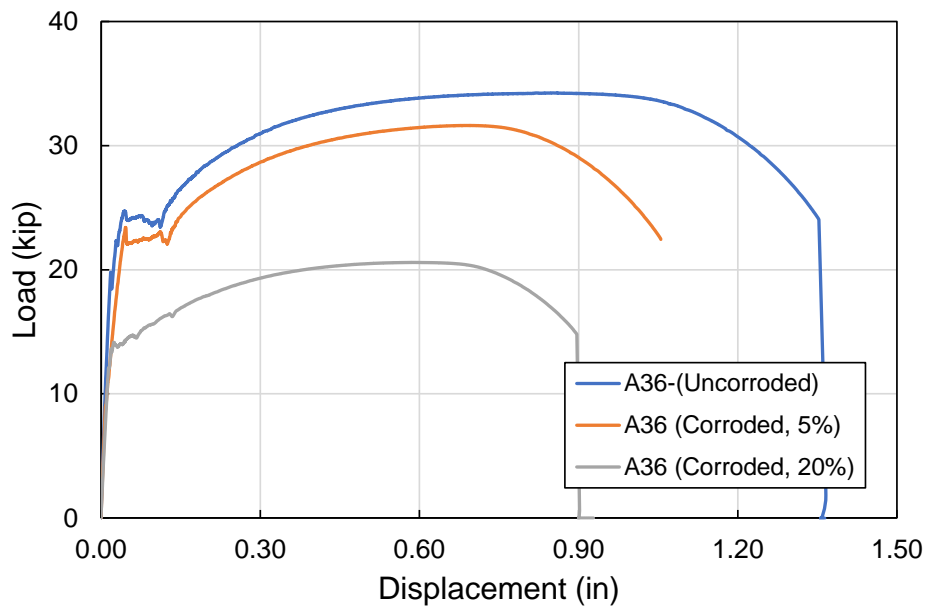

Figure 23. Load versus displacement curve for A36 specimens with and without corrosion
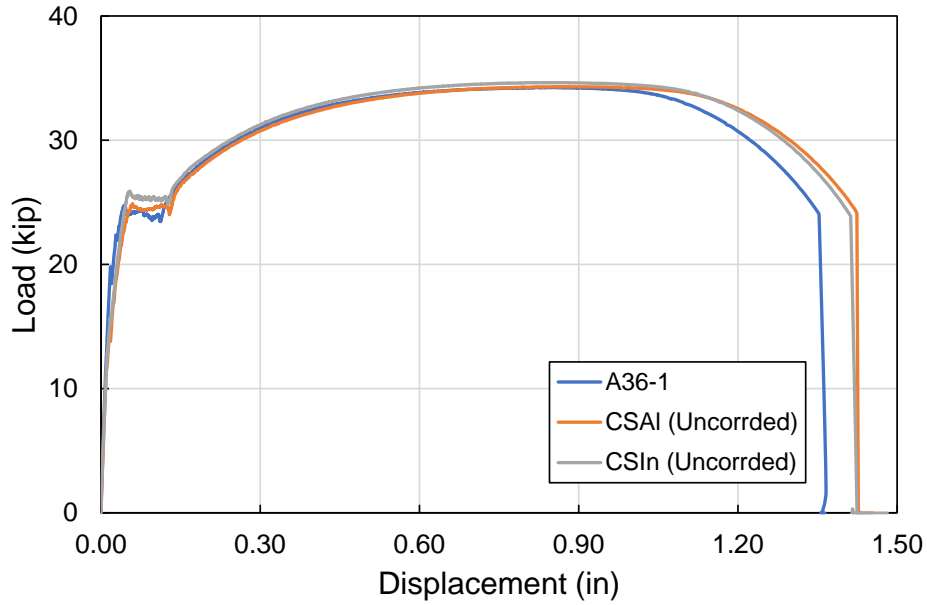
Figure 24. Load versus displacement curve for A36 specimens with and without corrosion cold-sprayed coatings
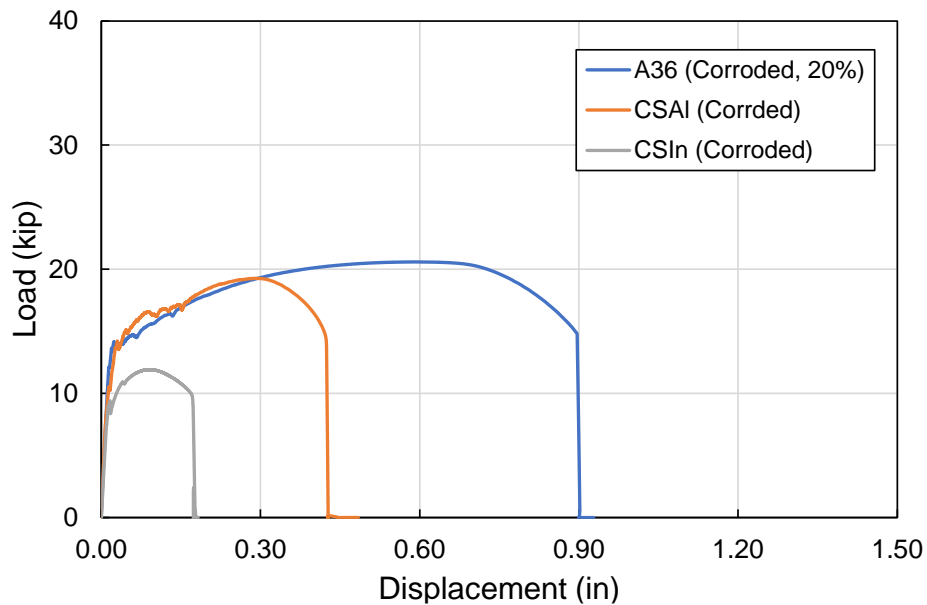
Figure 25. Load versus displacement curve for A36 corroded specimens with and without corrosion cold-sprayed coatings

It was noted that both the yield and tensile strength was decreased due to the corrosion as expected. It was also found from the comparison that the differences between the tensile behavior was found not to directly relate to the cold-sprayed coating. This might be because the coated layer was thin for these steel samples. However, the observed difference between the corroded A36 specimens with and without cold-sprayed coatings (i.e., aluminum and Inconel) in this study was not significant.

The fractured specimens for A36 coupons, A36 cold-sprayed coupons, and corroded A36 coupons with cold-sprayed coating are presented in Figure 26, Figure 27, and Figure 28, respectively. It can be noted from the experiments that the bonding between the substrate steel and the coating material seemed to be not adequate after the steel began to yield.

Figure 26. Fractured samples of the A36 coupons with and without cold-sprayed coating after tensile tests

Figure 27. Fractured samples of the corroded A36 coupons with aluminum cold-sprayed after tensile tests

Figure 28. Fractured samples of the corroded A36 coupons with inconel cold-sprayed after tensile tests

Furthermore, for corroded coupons as shown in the above figures, localized failure was noted, where it was near both ends of gripping areas. This was mainly because the corroded specimens coated with Inconel posed unexpected challenges. In particular, as shown in Figure 29, for some specimens the coating either cracked or "blisters" appeared.
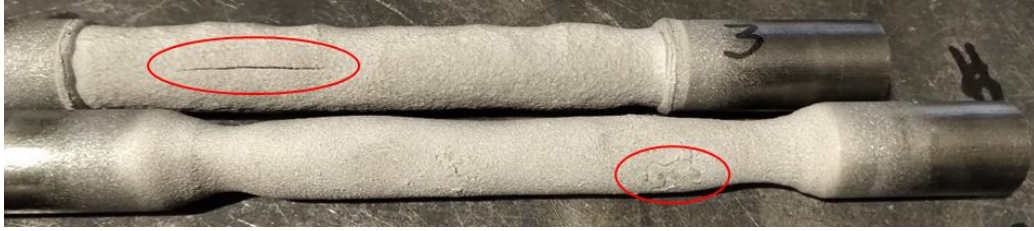
Figure 29. Corroded specimens after coating with Inconel: the upper specimen developed a crack in the deposit as it cooled down; the lower specimen showed "blistering"

Hardness Tests

Because of the curvature in bar specimens in this project, only the spherical indenter was able to accurately measure the hardness. Therefore, a conventional Rockwell hardness testing method was chosen for hardness measurements. Hardness readings were taken using a Leco Rockwell Hardness tester, as shown in Figure 30.

Figure 30. Rockwell hardness tester

A concave-surfaced sample holder was used due to the bar sample in this study. The mean Rockwell A hardness test results are calculated from three measurements and summarized in Table 9.

Table 9. Rockwell A hardness testing results

Specimen	Rockwell A hardness
CSIn	77.5
CSAl	11.2

Laboratory Test Summary and Conclusions

The experimental program was to investigate the mechanical performance of cold-sprayed steel coupons under tensile loads.

From the laboratory work, the following conclusions were made:

- It was found that the differences in tensile behavior among the cold-sprayed specimens were not directly related to the coating. This might be because the coated layer was thin for these steel samples.

- The bonding between the substrate steel and the coating material seemed to be inadequate after the steel began to yield.

- From the hardness testing, the cold-sprayed steel coupon coated with Inconel had a Rockwell A hardness value of 77.5. However, the Rockwell A hardness value of the cold-sprayed steel coupon coated with aluminum was found to be 1.2 because the aluminum coating significantly softened the material.

SUMMARY AND CONCLUSIONS

Summary

Cold gas dynamic spraying is a promising additive manufacturing technique in which metallic materials or alloy compounds are deposited onto the surface of a substrate. In CS, an inert gas such as helium or nitrogen is accelerated in a de Laval nozzle through an adiabatic expansion process (Koivuluoto and Vuoristo 2014). CS has mainly been used in the oil and gas industries to apply titanium on metallic substrates (Wang et al. 2007, Sun et al. 2008, Binder et al. 2010, Wong et al. 2011, Prisco et al. 2018). Due to the high price of titanium, one of the aims of the present project was to identify other metallic compounds with the desired corrosion resistance and mechanical performance to be deposited onto corroded steel members using the CS method.

This research project aimed to investigate the feasibility of using the CS method for the repair and retrofit of corroded steel members, especially in bridge structures. This study's outcome is a set of recommendations regarding the use of the cold spray technique in steel structures.

In this study, the experimental program was designed to evaluate the corrosion resistance of cold-sprayed coating on steel coupons. To this end, accelerated corrosion testing was conducted in accordance with ASTM G 31 on a variety of metals and alloys, and some were selected for further testing with cold-sprayed coating. Furthermore, the experimental program was designed to investigate the mechanical performance of cold-sprayed steel coupons under tensile loads.

Conclusions and Recommendations

From the accelerated corrosion testing, the following conclusions were made:

- For the 7-day testing period, the average loss was 4.5% for A36 steel, 5% for A1010 steel, and 10% for aluminum. For the cold-sprayed coupons, the average losses were 4.4% and 1.2% for the coupons coated with Inconel and aluminum, respectively.

- For the 14-day testing period, the average loss was 20% for A36 steel, while the average losses were significantly lower for the cold-sprayed coupons coated with Inconel and aluminum, 4.0% and 3.1%, respectively.

- A comparison of the two coating materials investigated revealed that the Inconel-coated bars had higher corrosion rates in both tests and appeared significantly more corroded than the aluminum-coated bars. The aluminum-coated bars had more consistent corrosion, lower corrosion rates, and less severe corrosion, making aluminum the more effective protective coating.

From the tensile and hardness testing, the following conclusions were made:

- It was found that the differences in tensile behavior among the cold-sprayed specimens were not directly related to the coating. This might be because the coated layer was thin for these steel samples.

- The bonding between the substrate steel and the coating material was found to be in need of attention.

- From the hardness testing, the cold-sprayed steel coupon coated with Inconel had a Rockwell A hardness value of 77.5. However, the Rockwell A hardness value of the cold-sprayed steel coupon coated with aluminum was found to be 11.2 because the aluminum coating significantly softened the material.

REFERENCES

Al-Mangour, B., P. Vo, R. Mongrain, E. Irissou, and S. Yue. 2013. Effect of Heat Treatment on the Microstructure and Mechanical Properties of Stainless Steel 316L Coatings Produced by Cold Spray for Biomedical Applications. *Journal of Thermal Spray Technology*, Vol. 23, No. 4, pp. 641–652.

Arabi, S., and B. Shafei. 2019. Multi-Stressor Fatigue Assessment of Steel Sign-Support Structures: A Case Study in Iowa. *Engineering Structures*, Vol. 200, No. 109721, pp. 1–11.

Arabi, S., B. Shafei, and B. Phares. 2019. Investigation of Fatigue in Steel Sign-Support Structures under Diurnal Temperature Changes. *Constructional Steel Research*, Vol. 153, pp. 286–297.

Arabi, S., B. Shafei, and B. Phares. 2018. Fatigue Analysis of Sign-Support Structures During Transportation under Road-Induced Excitations. *Engineering Structures*, Vol. 164, pp. 305–315.

Assadi, H., H. Kreye, F. Gärtner, and T. Klassen. 2016. Cold Spraying – A Materials Perspective. *Acta Materialia*, Vol. 116, pp. 382–407.

Bae, G., Y. Xiong, Y., S. Kumar, K. Kang, and C. Lee. 2009. General Aspects of Interface Bonding in Kinetic Sprayed Coatings. *Acta Materialia*, Vol.56, No. 17, pp. 4858–4868.

Bala, N., H. Singh, J. Karthikeyan, and S. Prakash. 2014. Cold Spray Coating Process for Corrosion Protection: A Review. *Surface Engineering*, Vol. 30, No. 6, pp. 414–421.

Binder, K., J. Gottschalk, M. Kollenda, F. Gärtner, and T. Klassen. 2010. Influence of Impact Angle and Gas Temperature on Mechanical Properties of Titanium Color Spray Deposits. *Journal of Thermal Spray Technology*, Vol. 20, pp. 234–242.

Borchers, C., T. Schmidt, F. Gärtner, and H. Kreye. 2008. High Strain Rate Deformation Microstructures of Stainless Steel 316L by Cold Spraying and Explosive Powder Compaction. *Applied Physics A*, Vol. 90, No. 3, pp. 517–526.

Bray, M., A. Cockburn, and W. O'Neill. 2009. The Laser-Assisted Cold Spray Process and Deposit Characterisation. *Surface and Coatings Technology*, Vol. 203, No. 19, pp. 2851–2857.

Coddet, P., C. Verdy, C. Coddet, F. Debray, and F. Lecouturier. 2015. Mechanical Properties of Thick 304L Stainless Steel Deposits Processed by He Cold Spray. *Surface and Coatings Technology*, Vol. 277, pp. 74–80.

Fernández, R., D. MacDonald, A. Nastić, B. Jodoin, B., A. Tieu, and M. Vijay. 2016. Enhancement and Prediction of Adhesion Strength of Copper Cold Spray Coatings on Steel Substrates for Nuclear Fuel Repository. *Journal of Thermal Spray Technology*, Vol. 25, No. 8, pp. 1577–1587.

Grujicic, M., J. Saylor, D. Beasley, W. DeRosset, and D. Helfritch. 2003. Computational Analysis of the Interfacial Bonding between Feed-Powder Particles and the Substrate in the Cold-Gas Dynamic-Spray Process. *Applied Surface Science*, Vol. 219, Nos. 3–4, pp. 211–227.

Hassani-Gangaraj, S. M., A. Moridi, and M. Guagliano. 2015. Critical Review of Corrosion Protection by Cold Spray Coatings. *Surface Engineering*, Vol. 31, No. 11, pp. 803–815.

Imperatore, S., Z. Rinaldi, and C. Drago. 2017. Degradation Relationships for the Mechanical Properties of Corroded Steel Rebars. *Construction and Building Materials*, Vol. 148, pp. 219–230.

Kim, K., M. Watanabe, K. Mitsuishi, K. Iakoubovskii, and S. Kuroda. 2009. Impact Bonding and Rebounding between Kinetically Sprayed Titanium Particle and Steel Substrate Revealed by High-Resolution Electron Microscopy. *Journal of Physics D: Applied Physics*, Vol. 42, No. 6, 065304, pp. 1–5.

Koivuluoto, H., and P. Vuoristo. 2014. Structure and Corrosion Properties of Cold Sprayed Coatings: A Review. *Surface Engineering*, Vol. 30, No. 6, pp. 404–413.

Li, W., H. Liao, G. Douchy, and C. Coddet. 2007. Optimal Design of a Cold Spray Nozzle by Numerical Analysis of Particle Velocity and Experimental Validation with 316L Stainless Steel Powder. *Materials and Design*, Vol. 28, No. 7, pp. 2129–2137.

Li, W. Y., J. Wang, H. Zhu, H. Li, and C. Huang. 2013. On Ultrahigh Velocity Micro-Particle Impact on Steels—A Single Impact Study. *Wear*, Vol. 305, Nos. 1–2, pp. 216–227.

Moridi, A., S. Hassani-Gangaraj, and M. Guagliano. 2013. A Hybrid Approach to Determine Critical and Erosion Velocities in the Cold Spray Process. *Applied Surface Science*, Vol. 273, pp. 617–624.

Olakanmi, E. O. and M. Doyoyo. 2014. Laser-Assisted Cold-Sprayed Corrosion- and Wear-Resistant Coatings: A Review. *Journal of Thermal Spray Technology*, Vol. 23, No. 5, pp. 765–785.

Oyinbo, S. T. and T-C. Jen. 2019. A Comparative Review on Cold Gas Dynamic Spraying Processes and Technologies. *Manufacturing Review*, Vol. 6, No. 25.

Prisco, U., A. Squillace, A. Astarita, and L. Carrino. 2018. Morphology of Titanium Coatings Deposited through Single Pass Cold Spraying. *Materials and Manufacturing Processes*, Vol. 33, No. 2, pp. 123–129.

Raoelison, R., C. Verdy, and H. Liao. 2017. Cold Gas Dynamic Spray Additive Manufacturing Today: Deposit Possibilities, Technological Solutions and Viable Applications. *Materials and Design*, Vol. 133, pp. 266–287.

Schmidt, T., F. Gaertner, and H. Kreye. 2009. New Developments in Cold Spray Based on Higher Gas and Particle Temperatures. *Journal of Thermal Spray Technology*, Vol. 15, No. 4, pp. 488–494.

Shi, W, B. Shafei, and B. Phares. 2021. Structural Capacity and Fatigue Performance of ASTM A709 Grade 50CR Steel. *Construction and Building Materials*, Vol. 270, No. 121379, pp. 1–11.

Shurbert-Hetzel, C., B. Shafei, and B. Phares. 2021. Performance of Steel Dynamic Message Sign-Support Structures in Extreme Wind Events. *Engineering Structures*, Vol. 237, No. 112086, pp. 1–15.

Silva, F., J. Bedoya, J., S. Dosta, N. Cinca, I. Cano, J. Guilemany, and A. Benedetti. 2016. Corrosion Characteristics of Cold Gas Spray Coatings of Reinforced Aluminum Deposited onto Carbon Steel. *Corrosion Science*, Vol. 114, pp. 57–71.

Spencer, K. and M. Zhang. 2011. Optimisation of Stainless Steel Cold Spray Coatings Using Mixed Particle Size Distributions. *Surface and Coatings Technology*, Vol. 205, pp. 5135–5140.

Spencer, K., D. Fabijanic, and M. Zhang. 2012. The Influence of Al2O3 Reinforcement on the Properties of Stainless Steel Cold Spray Coatings. *Surface and Coatings Technology*, Vol. 206, No. 14, pp. 3275–3282.

Stoltenhoff, T., H. Kreye, and H. J. Richter. 2002 An Analysis of the Cold Spray Process and Its Coatings. *Journal of Thermal Spray Technolo*gy, Vol. 11, pp. 542–550.

Sun, J., Y, Han, and K. Cui. 2008. Innovative Fabrication of Porous Titanium Coating on Titanium by Cold Spraying and Vacuum Sintering. *Materials Letters*, Vol. 62, Nos., 21–22, pp. 3623–3625.

Sundararajan, G., P. S. Phani, A. Jyothirmayi, and R. C. Gundakaram. 2008. The Influence of Heat Treatment on the Microstructural, Mechanical and Corrosion Behaviour of Cold Sprayed SS 316L Coatings. *Journal of Materials Science*, Vol. 44, No. 9, pp. 2320–2326.

Villa, M., S. Dosta, S., and J. Guilemany. 2013. Optimization of 316L Stainless Steel Coatings on Light Alloys Using Cold Gas Spray. *Surface and Coatings Technology*, Vol. 235, pp. 220–225.

Wang H. R., W. Y. Li, L. Ma, J. Wang, and Q. Wang. 2007. Corrosion Behavior of Cold Sprayed Titanium Protective Coating on 1Cr13 Substrate in Seawater. *Surface and Coatings Technology*, Vol. 201, Nos. 9–11, pp. 5203–5206.

Wong W., E. Irissou, A. N. Ryabinin, J. G. Legoux, and S. Yue. 2011. Influence of Helium and Nitrogen Gases on the Properties of Cold Gas Dynamic Sprayed Pure Titanium Coatings. *Journal of Thermal Spray Technology*, Vol. 20, pp. 213–226.

Yin S., X. Wang, W. Li, H. Liao, and H. Jie. 2012. Deformation Behavior of the Oxide Film on the Surface of Cold Sprayed Powder Particles. *Applied Surface Science,* Vol. 259, pp. 294–300.

Ziemian, C. W., M. M. Sharma, B. D. Bouffard, T. Nissley, and T. J. Eden. 2014. Effect of Substrate Surface Roughening and Cold Spray Coating on the Fatigue Life of AA2024 Specimens. *Materials and Design*, Vol. 54, pp. 212–221.

**THE INSTITUTE FOR TRANSPORTATION IS THE FOCAL POINT FOR TRANSPORTATION
AT IOWA STATE UNIVERSITY.**

InTrans centers and programs perform transportation research and provide technology transfer services for government agencies and private companies;

InTrans contributes to Iowa State University and the College of Engineering's educational programs for transportation students and provides K–12 outreach; and

InTrans conducts local, regional, and national transportation services and continuing education programs.